UC Santa Barbara
UC Santa Barbara Previously Published Works

Title

Multiscale simulation of ideal mixtures using smoothed dissipative particle dynamics

Authors

Petsev, Nikolai D
Leal, L Gary
Shell, M Scott

Multiscale simulation of ideal mixtures using smoothed dissipative particle dynamics

Nikolai D. Petsev, L. Gary Leal, and M. Scott Shell
Department of Chemical Engineering, University of California at Santa Barbara, Santa Barbara, California 93106-5080, USA

Smoothed dissipative particle dynamics (SDPD) [P. Español and M. Revenga, Phys. Rev. E **67**, 026705 (2003)] is a thermodynamically consistent particle-based continuum hydrodynamics solver that features scale-dependent thermal fluctuations. We obtain a new formulation of this stochastic method for ideal two-component mixtures through a discretization of the advection-diffusion equation with thermal noise in the concentration field. The resulting multicomponent approach is consistent with the interpretation of the SDPD particles as moving volumes of fluid and reproduces the correct fluctuations and diffusion dynamics. Subsequently, we provide a general *multiscale* multicomponent SDPD framework for simulations of molecularly miscible systems spanning length scales from nanometers to the non-fluctuating continuum limit. This approach reproduces appropriate equilibrium properties and is validated with simulation of simple one-dimensional diffusion across multiple length scales. © 2016 AIP Publishing LLC. [http://dx.doi.org/10.1063/1.4942499]

I. INTRODUCTION

Stochastic particle descriptions for mesoscale phenomena have become ubiquitous in simulation due to their ability to accurately reproduce hydrodynamic behavior over time and length scales beyond what is feasible in fully resolved molecular dynamics (MD). In this coarse-grained picture, the detailed underlying molecular structure is ignored and the problem domain is instead decomposed into a collection of fluid volumes or clusters of atoms/molecules, with appropriately chosen interparticle interactions between them such that desired thermodynamic and hydrodynamic properties of the original fluid are preserved. Coarse-grained particle descriptions of fluids are often obtained from a "bottom-up" perspective, where the coarse model is extracted from detailed molecular simulations or principles and features a smoother representation of the free energy landscape that allows for large time-stepping. Alternatively, it is possible to adopt a "top-down" approach and use a coarse-grained fluid description that ignores molecular detail altogether, such as the continuum transport equations. Degrees of freedom absent in the coarse model are approximated by introducing additional features (e.g., fluctuations of field variables).

Smoothed Dissipative Particle Dynamics (SDPD)[1] is one such particle-based top-down approach and has been applied to a number of phenomena, including pinned DNA in shear flow,[2] colloidal particles,[3] the flow of blood,[4] intravascular drug delivery,[5] suspensions,[6] and viscoelastic flows.[7,8] Thieulot *et al.*[9,10] developed a SDPD-like model for a phase-separating fluid mixture by introducing fluctuations through the GENERIC formalism[11–13] following a particle discretization of the appropriate continuum equations. In addition, Ellero *et al.*[8] used GENERIC to obtain a discretized advection-diffusion equation for a system of Hookean dumbbells in solvent. For the most part, however, SDPD has been limited to single-component systems or suspensions where dissolved particles are equal in size or larger than the SDPD particles (e.g., colloidal or polymeric systems). Multicomponent problems have also been considered in other types of particle-based mesoscale simulations,[14,15] although this is done in an *ad hoc* fashion where fluid volumes assume a unique identity (e.g., a particle in a two-component mixture is either type A or type B). This simple approach is easy to implement and qualitatively adequate in many cases, but not consistent with the interpretation of particles as fluid volumes, since a single particle in a homogeneous fluid mixture should contain some amount of solute and solvent. Therefore, a more rigorous extension of these kinds of particle solvers for solutions should instead include an additional variable associated with each fluid volume specifying the concentration of solute at the particle. Recently, Li *et al.* extended traditional particle-based solvers to advection-diffusion-reaction systems.[16] There have also been recent developments by Kordilla *et al.*,[17] who derived this type of single-scale multicomponent stochastic particle method through a direct particle discretization of the Landau-Lifshitz fluctuating hydrodynamics equations for mass and momentum transfer.[18–20]

In this paper, we take a different approach and instead develop a multicomponent SDPD model that provides an appropriate basis for multiscale simulation of hydrodynamic phenomena through the GENERIC formalism,[11–13] which guarantees thermodynamic consistency. SDPD and other particle-based fluid solvers are particularly attractive for designing multiscale simulation strategies that reduce computational cost through coarse-graining of select parts of the system, while retaining a high level of detail in others. This is motivated by an abundance of problems in molecular and interfacial physics that involve processes featuring multiple characteristic length scales. In particular,

there have been a number of studies describing approaches for coupling MD regions to continuum domains, which makes it possible to preserve molecular resolution where necessary and use a simpler, coarse-grained description where this level of detail is not required.[21–29] SDPD specifically has already been used in coupled MD-continuum simulations.[30] While there are a number of hybrid simulation approaches for single-component problems, developing general multiscale strategies for multicomponent systems remains a major challenge. Since SDPD has scale-dependent fluctuations, it is ideally suited for multiscale problems, and an approach for coupling two SDPD regions featuring different degrees of coarse-graining has been developed by Kulkarni *et al.*[31] Therefore, generalizing SDPD to multicomponent systems immediately allows for a novel approach to multiscale multicomponent simulation, which is the subject of this work. This kind of particle-based Lagrangian description offers an alternative to spatially adaptive approaches to solving the fluctuating hydrodynamics equations in the Eulerian frame.[32]

SDPD addresses a number of issues present in one of the most widespread bottom-up particle-based techniques, dissipative particle dynamics (DPD).[33,34] In DPD, the fluid is modeled as a collection of particles, where each particle is interpreted as a cluster of molecules that is locally at thermodynamic equilibrium. These mesoscopic fluid volumes interact with one another and evolve in time through a Langevin-type equation of motion; particles experience a soft repulsion as they approach along the line joining their centers, as well as pairwise viscous and random forces with magnitudes chosen in accordance with the fluctuation-dissipation (FD) theorem. This approach preserves Galilean invariance and conserves mass and momentum, giving rise to hydrodynamic behavior.[35] DPD has been applied to a wide range of problems, ranging from polymer solutions and melts[36–39] to the rheology of spherical and non-spherical colloids,[40–42] membranes,[43,44] surfactant monolayers,[45] and vesicles.[46,47] Atomistic interaction potentials, or ones obtained from inverse thermodynamic approaches,[48,49] can also be used in place of the softly repulsive conservative DPD force, i.e., the viscous and fluctuating DPD interactions also provide a basis for thermostatting a fluid in a non-equilibrium setting.[50–52] Despite great success in modeling a broad range of mesoscale phenomena, DPD suffers from a number of limitations. Fluid transport coefficients (e.g., bulk and shear viscosities) do not appear in the equations of motion and are related to the free parameters of the DPD model in an indirect fashion through kinetic theory.[53,54] Moreover, traditional DPD fixes the form of the conservative force and, in turn, the equation of state such that it is always quadratic in the fluid density.

These issues were resolved by Español and Revenga, who derived the so-called SDPD[1] starting from a particle discretization of the hydrodynamic equations known as smoothed particle hydrodynamics, or SPH.[55–57] SPH is a continuum approach originally developed for modeling astrophysical problems and later modified for simulation of flows in the low Reynold's number limit.[58] Here, the fluid is approximated as a collection of Lagrangian particles that evolve in time according to an equation of motion

obtained from an interpolation theory discretization of the Navier-Stokes equations. By introducing fluctuations into the hydrodynamic variables of the SPH equations in accordance with the second law, Español and Revenga obtain a general model for fluids at the mesoscale that is rigorously derived from a top-down perspective. The resulting approach (SDPD) corresponds to a particle discretization of the Landau-Lifshitz Navier-Stokes equations and offers a number of advantages over traditional particle-based mesoscale techniques such as DPD.[1] Since the basis for SDPD is the continuum hydrodynamic equations, transport coefficients are naturally included and appear in the final equations of motion, and it is possible to use an arbitrary equation of state for calculating the pressure distribution. Importantly, the characteristic length scale in SDPD is properly defined and determined by a parameter known as the "smoothing length." For systems involving small smoothing lengths, the corresponding fluid particles are very small and therefore subject to large thermal fluctuations. Similarly, in the limit of large smoothing lengths and hence large particles, fluctuations disappear altogether and the deterministic SPH equations of motion are recovered.

We follow the approach in Ref. 1 in this work and start from a continuum, top-down perspective to derive a discrete particle model for ideal binary mixtures where the concentration field is specified by defining a concentration associated with each fluid particle. Unlike Ref. 17, we introduce thermal noise through the GENERIC framework and obtain a model that presents a convenient basis for multiscale simulation. Although this approach is only valid for ideal mixtures, it is still useful for a host of problems, such as biological and drug delivery applications where the ideal assumption is valid due to the dilute concentrations. In using the fluctuating hydrodynamic equations for two-component solutions as a basis, we obtain a model where a particle is no longer limited to the discrete choice of assuming identity A or B, but rather has associated with it a variable indicating the mass fraction of solute contained in the particle volume. We reconcile this multicomponent SDPD approach with existing multiscale techniques and provide a general SDPD formalism for multiscale multicomponent simulation. In Section II, we derive a fluctuating concentration smoothed particle model for a quiescent system (i.e., in the absence of any flow fields). In Section III, the model is generalized for systems with flows and fluctuations in the velocity field, and in Section V, we describe how this method is used in multiscale simulation. The approach is validated through some simple multiscale equilibrium and non-equilibrium benchmark problems in Sections V and VI.

II. FLUCTUATING CONCENTRATION MODEL DERIVATION

We first develop a mass diffusion model for a collection of SDPD particles at a constant temperature with fixed positions. The model is for a two-component incompressible fluid in the ideal mixing limit. We then extend this approach in Section III to cases with momentum transfer featuring thermal noise in the velocity field, in which particles are not stationary. The diffusion equation in the Lagrangian frame and in the absence

of temperature gradients is given by[59]

$$\frac{d\Phi}{dt} = \frac{1}{\rho} \nabla \cdot (D\nabla\Phi). \tag{1}$$

Here, D is the diffusion coefficient for the solute and is defined in terms of units $ML^{-1} t^{-1}$, the concentration Φ is a mass fraction (hence, dimensionless), and ρ is the total mass density of the solute-solvent mixture. The time derivative on the left-hand side denotes the material derivative, although for the present case where particle positions are fixed and there are no velocities in the system, it is equivalent to a partial derivative with respect to time.

Discretizing Eq. (1) through an interpolant function W, we obtain the SPH approximation for the diffusion equation,[60]

$$m_i\frac{d\Phi_i}{dt} = 2D\sum_{j=1}^{N}\frac{m_im_j}{\rho_i\rho_j}\left(\frac{1}{|\mathbf{r}_{ij}|}\frac{\partial W_{ij}}{\partial r_{ij}}\right)\Phi_{ij}. \tag{2}$$

Here, m_i is the mass of the ith particle, ρ_i is the density of the ith particle, $\Phi_{ij} \equiv \Phi_i - \Phi_j$, and $\mathbf{r}_{ij}$ is the relative position vector for the particles i and j, $\mathbf{r}_{ij} \equiv \mathbf{r}_i - \mathbf{r}_j$. W_{ij} is the smoothing function (described below). For simplicity, transport coefficients are assumed to be uniform throughout the system; for the more general case where the diffusion constant varies in space, the quantity $2D$ in Eq. (2) is brought inside the summation and replaced with $4D_iD_j/(D_i + D_j)$, where D_i is the diffusion constant for the ith particle.[60]

The density at each particle can be updated from a discretization of the continuity equation or by performing the following summation at each time-step:

$$\rho(\mathbf{r}_i) = \sum_{j=1}^{N} m_j W(\mathbf{r}_i - \mathbf{r}_j, h). \tag{3}$$

In this equation, h is the smoothing length, a parameter that controls the size of the particles and hence the length scale for the fluid. The smoothing kernel $W(\mathbf{r}_{ij}, h) \equiv W_{ij}$ is a normalized bell-shaped function with compact support. One possibility is a cubic spline, which is used for all numerical tests presented in this work,[31,57,61]

$$W_{ij}(q) = \frac{1}{\pi h^3}\begin{cases} 1 - \frac{3}{2}q^2 + \frac{3}{4}q^3, & 0 \le q < 1 \\ \frac{1}{4}(2-q)^3, & 1 \le q < 2 \\ 0, & q \ge 2 \end{cases}. \tag{4}$$

Here, $q = r_{ij}/h$.

The objective of this section is to introduce scale-dependent thermal noise in the concentration field, which is achieved through the GENERIC[11–13] framework. In GENERIC, the system dynamics are governed by the following stochastic differential equations (SDEs):

$$dx = \left[L \cdot \frac{\partial E}{\partial x} + M \cdot \frac{\partial S}{\partial x} + k_B\frac{\partial}{\partial x} \cdot M\right]dt + d\tilde{x}. \tag{5}$$

Here, x denotes the independent variables that completely describe the system; in this case, it is fully specified by the set of particle positions and the respective concentration at each particle, $x = \{\mathbf{r}_i, \Phi_i, i = 1, \ldots, N\}$. M is the dissipative matrix, a positive semidefinite linear operator that acts on the entropy

gradients to generate the irreversible dynamics. E denotes the total system energy and L is an antisymmetric operator that translates energy gradients into reversible dynamics. For the present case, this term is zero since the processes under consideration are purely irreversible; this will not be the case in Section III where fluid motion is considered. In the above equation, $d\tilde{x}$ is the stochastic contribution. The term $k_B(\partial/\partial x) \cdot M$ appears due to the Itô interpretation of the stochastic integral.[11,13]

For a two-component ideal mixture, the entropy of mixing is simply

$$S_i = -\left(\frac{m_i}{m_0}\right)k_B[\Phi_i \ln \Phi_i + (1 - \Phi_i)\ln(1 - \Phi_i)], \tag{6}$$

where m_0 denotes the mass of a single atom. Hence $m_i/m_0 = N_i$, where N_i is the number of atoms or molecules inside the ith SDPD particle. The driving force for an irreversible process is given by the entropy gradient,

$$\frac{\partial S_i}{\partial \Phi_i} = -\left(\frac{m_i}{m_0}\right)k_B \ln\left(\frac{\Phi_i}{1 - \Phi_i}\right). \tag{7}$$

Next, we postulate a form for the noise term. If we assume pairwise fluxes between particles, the simplest possible choice for introducing noise in a scalar field is

$$m_i d\tilde{\Phi}_i = \sum_{j=1}^{N} G_{ij} dV_{ij}. \tag{8}$$

In this expression, dV_{ij} is an increment of the Wiener process with the antisymmetry $dV_{ij} = -dV_{ji}$, and G_{ij} is the noise amplitude, which is symmetric under exchange of particles i and j, $G_{ij} = G_{ji}$. In practice, dV_{ij} is approximated using a randomly generated number drawn from a normal distribution with unit variance and zero mean, $dV_{ij} \sim \sqrt{\Delta t}N(0,1)$. Here, Δt is the simulation time-step magnitude. The above symmetries ensure that the amount of solute is a conserved quantity, i.e.,

$$\sum_{i=1}^{N} m_i d\tilde{\Phi}_i = 0. \tag{9}$$

The FD theorem relates the noise in Eq. (8) to the dissipative matrix M. For any fluctuating state variable x, the FD theorem can be written as $d\tilde{x}d\tilde{x}^T = 2k_BMdt$. Thus, we use the FD theorem to write the ijth component of the dissipative matrix as

$$M_{ij} = \frac{d\tilde{\Phi}_i d\tilde{\Phi}_j}{2k_Bdt}. \tag{10}$$

We substitute the postulated noise terms [Eq. (8)] into Eq. (10) and write M_{ij} in terms of the noise amplitude G_{ij},

$$m_im_j\frac{d\tilde{\Phi}_i d\tilde{\Phi}_j}{dt} = \delta_{ij}\sum_{j'=1}^{N} G_{ij'}G_{jj'} - G_{ij}^2. \tag{11}$$

Here, we have assumed delta correlated noise by applying the mnemotechnical Itô rule $dV_{ii'}dV_{jj'} = [\delta_{ij}\delta_{i'j'} - \delta_{ij'}\delta_{i'j}]dt$.[1,62]

For discrete particle models, the dot operator in Eq. (5) corresponds to a sum over particle indices. Hence, the stochastic dynamics for the concentration field are

governed by

$$\frac{d\Phi_i}{dt} = \sum_j \frac{d\tilde{\Phi}_i d\tilde{\Phi}_j}{2k_B dt} \left(\frac{\partial S_j}{\partial \Phi_j} \right). \quad (12)$$

All the quantities on the right-hand side of this expression are known. Substituting Eqs. (7) and (11), we arrive at the following evolution equation:

$$m_i \frac{d\Phi_i}{dt} = -\frac{1}{2m_0} \sum_{j=1}^N G_{ij}^2 \left[\ln\left(\frac{\Phi_i}{\Phi_j}\right) + \ln\left(\frac{1-\Phi_j}{1-\Phi_i}\right) \right]. \quad (13)$$

In order to compare this with the discretized diffusion equation [Eq. (2)], we modify Eq. (13) by first writing

$$\ln\left(\frac{\Phi_i}{\Phi_j}\right) = \frac{1}{2}\ln\left(\frac{\Phi_i}{\Phi_j}\right) - \frac{1}{2}\ln\left(\frac{\Phi_j}{\Phi_i}\right). \quad (14)$$

Linearizing the logarithmic terms, $\ln\left(\Phi_i/\Phi_j\right) \approx \Phi_i/\Phi_j - 1$, and recombining them,

$$\ln\left(\frac{\Phi_i}{\Phi_j}\right) \approx \frac{1}{2}\left(\frac{1}{\Phi_i} + \frac{1}{\Phi_j}\right)\Phi_{ij}. \quad (15)$$

Here, it is assumed that Φ_i/Φ_j is close to unity, i.e., that local concentration gradients and deviations from equilibrium are small. The linearization in Eq. (15) is applied to both logarithmic terms in Eq. (13), which gives the following approximation after some algebra:

$$m_i \frac{d\Phi_i}{dt} = -\frac{1}{4m_0} \sum_{j=1}^N G_{ij}^2 \left(\frac{\Theta_i + \Theta_j}{\Theta_i \Theta_j}\right)\Phi_{ij}, \quad (16)$$

where we have defined $\Theta_i = \Phi_i(1 - \Phi_i)$. For fluctuation-dissipation to hold, this equation governing the dissipation of the stochastic noise must be equivalent to the discretized diffusion equation. Hence, by comparing this expression to Eq. (2), we find that the following equality must be satisfied:

$$\frac{2Dm_i m_j}{\rho_i \rho_j}\left(\frac{1}{|\mathbf{r}_{ij}|}\frac{\partial W_{ij}}{\partial r_{ij}}\right) = -\frac{1}{4m_0}\left(\frac{\Theta_i + \Theta_j}{\Theta_i \Theta_j}\right)G_{ij}^2. \quad (17)$$

Solving for the noise magnitude term G_{ij},

$$G_{ij} = \left[-\frac{8Dm_0 m_i m_j}{\rho_i \rho_j}\left(\frac{\Theta_i \Theta_j}{\Theta_i + \Theta_j}\right)\frac{1}{|\mathbf{r}_{ij}|}\frac{\partial W_{ij}}{\partial r_{ij}} \right]^{1/2}. \quad (18)$$

This is the SDPD discretized form of the noise amplitude for the stochastic flux in the Landau-Lifshitz Navier-Stokes equations for a binary mixture, $G = \sqrt{2m_0 D\Phi(1-\Phi)}$.[63]

Finally, we compute the term in Eq. (5) involving the divergence of the dissipative matrix, $k_B(\partial/\partial x) \cdot M$, which arises due to the Itô interpretation of the stochastic differential equations. Calculating the divergence of the dissipative matrix is generally undesirable,[13] although since the model features multiplicative noise, including this additional term may be important. Hence, we calculate this term from

$$k_B \sum_j \frac{\partial}{\partial \Phi_j}\frac{d\tilde{\Phi}_i d\tilde{\Phi}_j}{2k_B dt} = \frac{1}{2m_i}\sum_j \frac{1}{m_j}\frac{\partial}{\partial \Phi_j}$$
$$\times\left(\delta_{ij}\sum_{j'}G_{ij'}G_{jj'} - G_{ij}^2\right). \quad (19)$$

Applying the delta function and simplifying, this reduces to

$$= \frac{1}{2m_i}\sum_j\left(\frac{1}{m_i}\frac{\partial G_{ij}^2}{\partial \Phi_i} - \frac{1}{m_j}\frac{\partial G_{ij}^2}{\partial \Phi_j}\right). \quad (20)$$

After substituting Eq. (18) into Eq. (20) and differentiating, it is possible to write the final SDEs governing the concentration field including the Itô term,

$$m_i d\Phi_i = 2D\sum_{j=1}^N (1 - g_{ij})\frac{m_i m_j}{\rho_i \rho_j}\left(\frac{1}{|\mathbf{r}_{ij}|}\frac{\partial W_{ij}}{\partial r_{ij}}\right)\Phi_{ij}dt + m_i d\tilde{\Phi}_i. \quad (21)$$

Eq. (21) is the discretized form of Eq. (1) with fluctuations in the concentration field. The noise term is described by Eq. (8) with amplitude given by Eq. (18). In the above equation, we have defined the following quantity:

$$g_{ij} = 2m_0\left[\frac{(1-2\Phi_i)m_j\Theta_j^2 - (1-2\Phi_j)m_i\Theta_i^2}{m_i m_j(\Theta_i + \Theta_j)^2(\Phi_i - \Phi_j)}\right]. \quad (22)$$

Note that this contribution to the governing equation scales inversely with particle mass. Hence, for large SDPD particles, it is much smaller than the other terms and usually negligible. For example, in Secs. IV–VI, we perform tests with particles having masses such that g_{ij} is a hundred times smaller than the irreversible term in Eq. (21). Moreover, the SDPD particles cannot be too small or the continuum assumption breaks down, and thus this term's influence will typically be minor relative to the rest. Hence, in all of the numerical tests presented in this paper, we ignore this contribution (i.e., we assume $g_{ij} \approx 0$).

III. SDPD MODEL FOR TWO-COMPONENT IDEAL MIXTURE WITH FLOW

We now consider the more general case when particles are allowed to translate due to flow fields in the system. In the presence of fluid motion, the positions of the SDPD particles evolve according to

$$\frac{d\mathbf{r}_i}{dt} = \mathbf{v}_i. \quad (23)$$

The velocity $\mathbf{v}_i$ can be determined from the momentum equation in the Lagrangian description,[59]

$$\rho\frac{d\mathbf{v}}{dt} = -\nabla p + \eta\nabla^2\mathbf{v} + \left(\zeta + \frac{\eta}{3}\right)\nabla\nabla \cdot \mathbf{v}. \quad (24)$$

Here, p denotes the pressure distribution, and η and ζ are the shear and bulk viscosities, respectively. In discretized form, this equation becomes[1]

$$m_i\frac{d\mathbf{v}_i}{dt} = -\sum_{j=1}^N m_i m_j\left(\frac{p_i}{\rho_i^2} + \frac{p_j}{\rho_j^2}\right)\frac{\partial W_{ij}}{\partial r_{ij}}\mathbf{e}_{ij}$$
$$+ \left(\frac{5\eta}{3} - \zeta\right)\sum_{j=1}^N \frac{m_i m_j}{\rho_i \rho_j}\left(\frac{1}{|\mathbf{r}_{ij}|}\frac{\partial W_{ij}}{\partial r_{ij}}\right)\mathbf{v}_{ij}$$
$$+ 5\left(\frac{\eta}{3} + \zeta\right)\sum_{j=1}^N \frac{m_i m_j}{\rho_i \rho_j}\left(\frac{1}{|\mathbf{r}_{ij}|}\frac{\partial W_{ij}}{\partial r_{ij}}\right)(\mathbf{v}_{ij} \cdot \mathbf{e}_{ij})\mathbf{e}_{ij}. \quad (25)$$

As before, transport coefficients are assumed constant for simplicity.

The expression governing the evolution of the concentration field remains unchanged from Section II since the particles are now free to move, and velocities determined from Eq. (25) are included in the material derivative of the equation for the solute transfer, Eq. (21). Equilibrium fluctuations in concentration and velocity are statistically independent,[64] hence we do not need to impose any correlation between velocity and concentration in the postulated form for the noise of those quantities. Thus, the appropriate form for the velocity noise for an ideal two-component system with flow at constant temperature is the same as for the single-component case,[1,62]

$$m_i d\tilde{\mathbf{v}}_i = \sum_{j=1}^{N} \left(A_{ij} d\hat{\mathbf{W}}_{ij} + B_{ij} \frac{1}{3} \mathrm{tr}\left[d\mathbf{W}_{ij} \right] \mathbf{I} \right) \cdot \mathbf{e}_{ij}. \quad (26)$$

In this expression, $d\mathbf{W}_{ij}$ is a tensorial generalization of the Wiener process and $d\hat{\mathbf{W}}_{ij}$ is the traceless, symmetric part of $d\mathbf{W}_{ij}$, $d\hat{W}_{ij}^{\alpha\beta} = \frac{1}{2} \left[dW_{ij}^{\alpha\beta} + dW_{ij}^{\beta\alpha} \right] - \frac{\delta^{\alpha\beta}}{3} \mathrm{tr}\left[d\mathbf{W}_{ij} \right]$. In non-equilibrium systems, advection of concentration due to velocity fluctuations in the fluid can lead to long-ranged correlations between fluctuations in concentration and velocity, which is responsible for the so-called giant fluctuation phenomenon.[65,63] This effect is naturally incorporated into Lagrangian fluctuating particle models since the velocity that appears in the material derivative of Eq. (21) includes the stochastic contribution.[17]

The noise magnitudes for the fluctuations in the velocity field are given by[1]

$$A_{ij} = \left[-\frac{4 m_i m_j k_B T}{\rho_i \rho_j} \left(\frac{5\eta}{3} - \zeta \right) \frac{1}{|\mathbf{r}_{ij}|} \frac{\partial W_{ij}}{\partial r_{ij}} \right]^{1/2},$$

$$B_{ij} = \left[-\frac{4 m_i m_j k_B T}{\rho_i \rho_j} \left(\frac{5\eta}{3} + 8\zeta \right) \frac{1}{|\mathbf{r}_{ij}|} \frac{\partial W_{ij}}{\partial r_{ij}} \right]^{1/2}. \quad (27)$$

The final SDE for the velocity field is[1]

$$\begin{aligned}
m_i d\mathbf{v}_i = &-\sum_{j=1}^{N} m_i m_j \left(\frac{p_i}{\rho_i^2} + \frac{p_j}{\rho_j^2} \right) \frac{\partial W_{ij}}{\partial r_{ij}} \mathbf{e}_{ij} dt \\
&+ \left(\frac{5\eta}{3} - \zeta \right) \sum_{j=1}^{N} (1 - d_{ij}) \frac{m_i m_j}{\rho_i \rho_j} \left(\frac{1}{|\mathbf{r}_{ij}|} \frac{\partial W_{ij}}{\partial r_{ij}} \right) \mathbf{v}_{ij} dt \\
&+ 5 \left(\frac{\eta}{3} + \zeta \right) \sum_{j=1}^{N} (1 - d_{ij}) \frac{m_i m_j}{\rho_i \rho_j} \left(\frac{1}{|\mathbf{r}_{ij}|} \frac{\partial W_{ij}}{\partial r_{ij}} \right) \\
&\times (\mathbf{v}_{ij} \cdot \mathbf{e}_{ij}) \mathbf{e}_{ij} dt + m_i d\tilde{\mathbf{v}}_i, \quad (28)
\end{aligned}$$

where

$$d_{ij} = \frac{k_B}{4} \left(\frac{1}{C_i} + \frac{1}{C_j} \right). \quad (29)$$

Once again, the term arising from the divergence of the dissipative matrix scales inversely with an extensive quantity (in this case, the extensive heat capacity) and hence becomes negligible for large SDPD particles. This term is also not included in the present calculations since we only consider situations where particles are massive and this contribution

is small. For the cases considered in this paper, it is not necessary to solve the entropy equation since it is decoupled from the equations of mass and momentum transfer at constant temperature.

Solid surfaces are treated in SDPD using virtual particles frozen on a lattice, and Dirichlet boundary conditions are imposed using the approach of Morris et al.,[58] where dissipative and random interactions between fluid and wall particles are modified in order to enforce the correct boundary values for the fields. For fluid-wall particle pair interactions, the distance of the fluid particle from the wall d_f and the distance of the virtual particle from the wall boundary d_w are calculated. Next, we calculate a factor β from

$$\beta = 1 + \frac{d_w}{d_f}. \quad (30)$$

This factor is used to rescale the dissipative terms in both the momentum and diffusion equations, ensuring the solution for the concentration and velocity assumes the correct values at the interface. For every pair interaction, this is equivalent to extrapolating the fluid particle's concentration and velocity across the interface and assigning values to the wall particle such that boundary conditions are satisfied. Note that the stochastic terms are rescaled by $\sqrt{\beta}$ rather than β in order to yield the correct fluctuation-dissipation balance.

IV. EQUILIBRIUM PROPERTIES OF FLUID MIXTURE

First, it is necessary to ensure that this model yields the appropriate fluctuations at equilibrium. SDPD particles have constant mass, but do exchange solute and solvent with their neighbors. Therefore, solute and solvent exchange between particle pairs are not independent, and if a particle loses some amount of solute to a neighbor, it must gain the same amount of solvent in order to conserve its mass. The variance of the solute fluctuations at equilibrium for a fluid volume with a constant mass constraint is obtained from a derivation similar to that in Ref. 64. The resulting expression for the concentration variance in a collection of SDPD particles each having dimensionless mass m/m_0 is given by

$$\left\langle (\Delta\Phi)^2 \right\rangle = \frac{m_0 \langle\Phi\rangle (1 - \langle\Phi\rangle)}{m}. \quad (31)$$

In the following simulations, we choose non-dimensional units such that the mass of a single molecule or atom is unity ($m_0 = 1$). This implies that the dimensionless mass m of a SDPD fluid volume equals the number of molecules N_0 that it contains, $N_0 = m$. Hence, a particle with mass $m = 100$ can be interpreted as a cluster or fluid volume comprised of 100 fluid atoms or molecules.

To evaluate equilibrium fluctuations in the new model, we consider two cases: (1) quiescent fluid at equilibrium with fluctuations in the concentration field alone, as described in Section II and (2) quiescent fluid at equilibrium with fluctuations in both concentration and velocity (described in Section III). In the first case, particles exist on a cubic lattice and their positions do not evolve in time. As a model fluid, we choose parameters that mimic a simple Lennard-Jones-like liquid, and all values are reported in reduced Lennard-Jones

units using the convention described in Refs. 30 and 31. According to Eq. (31), the concentration fluctuations are affected by the degree of coarse-graining (i.e., the SDPD particle mass) and the average concentration in the system. Hence, we vary these two parameters and perform equilibrium simulations to ensure that we obtain the correct distribution of concentrations for all cases. The particle masses considered are $m = 25$, 100, and 200 (with corresponding smoothing lengths $h = 3.75$, 6.00, and 7.50, respectively). The average concentrations tested for each case are $\langle \Phi \rangle = 0.25$, 0.50, and 0.75. For the $m = 25$ case, particles are initialized on an $8 \times 8 \times 8$ cubic lattice inside a box with dimensions of $25 \times 25 \times 25$ and periodic boundary conditions in all directions. For the simulations with particles masses $m = 100$, 1000 particles are initially placed on a $10 \times 10 \times 10$ lattice inside a periodic $50 \times 50 \times 50$ region. Finally, for the $m = 200$ case, we initialize an $8 \times 8 \times 8$ cubic lattice of particles inside a box with size $50 \times 50 \times 50$. The system temperature is $T = 1.0$ and the mass density is $\rho = 0.8$. For scenario (2), we also solve the momentum equation and choose $\zeta = 0.9$[66] and $\eta = 1.9$[67] for the viscosities. For convenience, the diffusion constant is assumed constant and set to unity ($D = 1.0$).

Fluid thermodynamic properties are determined by the choice of equation of state, which is an input parameter in SPH and SDPD. In these smoothed particle techniques, fluid motion is driven by local density gradients. Therefore, incompressible flows are typically approximated by choosing a quasi-incompressible equation of state that leads to large pressure gradients for small density perturbations. The equation of state is constructed such that density variations are small (it is recommended that density fluctuations remain within 3% of the target density[58]), while still allowing for practical time-step magnitudes. Presently, we choose $p_i = \rho_i c_s^2$,[31,56,57] where the speed of sound is $c_s = 5.0$,[31] giving average particle density fluctuations within 1.1% of the desired value for all tested fluid resolutions. The selected smoothing kernel is the cubic spline [Eq. (4)]. The Euler-Maruyama integrator[68] with a time-step of $\Delta t = 0.001$ is used for time-integration for case 1, where we have fixed particles' positions. For case 2, the same time-step is used and particle positions are evolved in time using a modified velocity-Verlet algorithm commonly used for DPD simulations,[17,69] where the concentration field is updated at the same points during the integration process as the velocity. The system is equilibrated for 1×10^6 time-steps, and the averaging is over 5×10^6 time-steps.

In Figure 1, the distribution of fluctuations determined from the SDPD simulations at three different average concentrations is compared to the analytical result, given by Gaussian distributions with the variance of Eq. (31). For clarity, we only show results for the fixed-position tests (case 1). The results for the runs where particles are allowed to move are indistinguishable from the fixed-position case as expected, since fluctuations in velocity and concentration are statistically independent at equilibrium. For all tests, the numerical calculations show excellent agreement with the analytical result. The time-averaged variance for the $\langle \Phi \rangle = 0.25$ SDPD simulations is within 0.8% of the theoretical result for the case with $m = 200$. The error in the variance for the cases with $m = 100$ and $m = 25$ is 1.7% and 6.5%, respectively. For
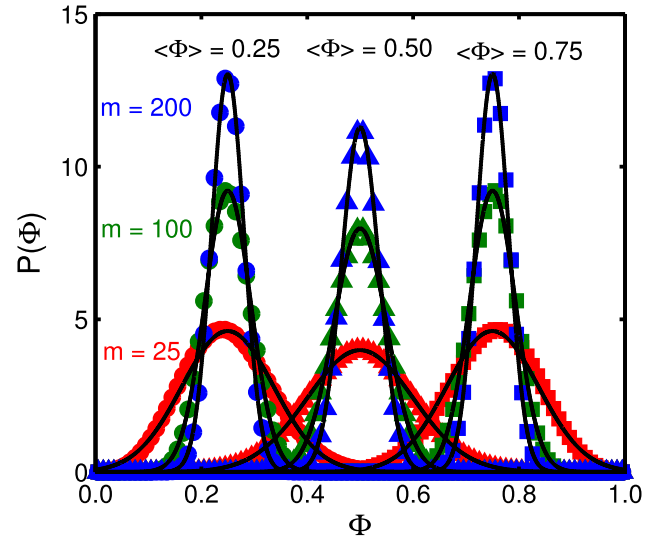

FIG. 1. Concentration probability distributions obtained from simulations using multicomponent SDPD (colored markers) as compared to the analytical result (black curves), given by a Gaussian with variance given by Eq. (31). Solutions with three different average concentrations are simulated, $\langle \Phi \rangle = 0.25$ (circle markers), 0.50 (triangles), and 0.75 (squares). For each concentration, we also consider three different particle masses, $m = 25$ (red markers), 100 (green), and 200 (blue). The results shown are for the fixed-position tests; simulation results for the case where particle positions evolve in time do not show any appreciable difference and are omitted for clarity.

the simulations with $\langle \Phi \rangle = 0.50$, the error in the distribution variance is 0.5% for the $m = 200$ case, 1.1% for $m = 100$, and 4.0% for $m = 25$. These errors are further reduced by decreasing the time-step.

We find that low order integrators such as Euler-Maruyama lead to precision issues if an insufficiently small time-step is used. Concentration cannot assume negative values (or values greater than one), and thus the distribution of concentrations becomes increasingly asymmetric with values of the average concentration approaching zero or unity. This is more prominent for situations involving very small SDPD particles since fluctuations become very large and the distribution of concentrations becomes very broad. A low-order integrator may not be sufficiently accurate to prevent fluctuations that lead to unphysical concentrations ($\Phi_i < 0$ or $\Phi_i > 1$). One possible approach to resolve these kinds of issues when dealing with smaller SDPD particles and dilute concentrations is to use an adaptive time-step integrator for propagating concentrations and/or velocities in time. This can be rigorously implemented through use of a Brownian tree algorithm.[70] With this algorithm, it is possible to detect unphysical concentrations and dynamically reduce the time-step as needed while preserving the original Brownian trajectory of the particle concentrations. For the present work, we simply choose an appropriately small time-step to avoid numerical difficulties.

V. MULTISCALE MULTICOMPONENT SDPD

In this section, the multicomponent approach outlined in Sections II and III is generalized to a multiscale simulation approach using the formulation of Kulkarni *et al.*[31] A similar
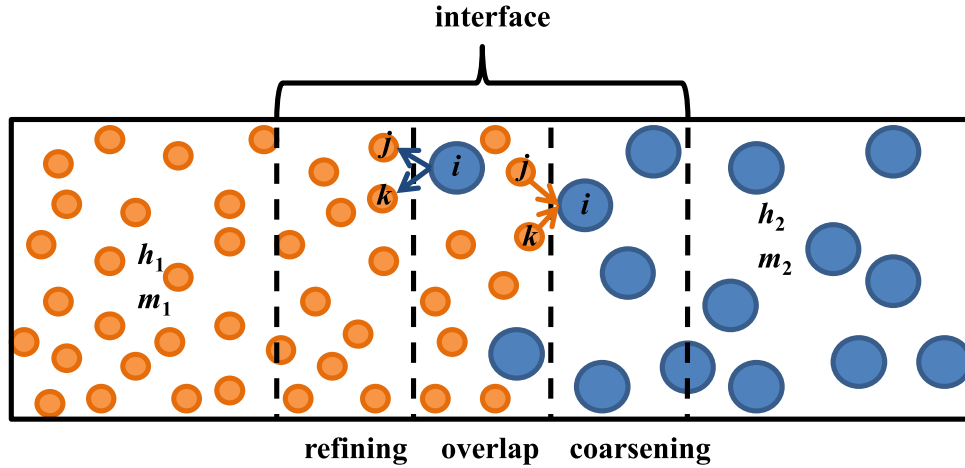
FIG. 2. Depiction of the multiscale SDPD simulation interface region between fluids with different resolutions. The "fine" SDPD fluid has smoothing length and mass h_1 and m_1, respectively. The "coarse" fluid in this example has a smoothing length of h_2 and mass of $m_2 = 2m_1$. The interface is divided into three parts: (1) refining, (2) overlap, and (3) coarsening subdomains. Once a large particle crosses into the refining region, it splits into two small SDPD particles each having half the mass of the parent particle. When a small particle crosses into the coarsening region, it is combined with another nearby particle into a large one. Large and small particles coexist within the overlap domain.

method has been developed for bridging regions featuring traditional DPD particles with a coarse-grained DPD particle description.[71] In both of these works, separate parts of the simulation box contain SDPD/DPD fluids with varying levels of detail. For the SDPD case, the resolution is determined by the smoothing length parameter that controls the particle masses, and hence the magnitude of the fluctuations. Therefore, it is possible to couple a finely resolved SDPD particle region (where particles have smoothing length h_1 and some corresponding mass m_1) to a more coarse one (containing particles with $h_2 > h_1$ and $m_2 > m_1$) by carefully constructing an interface between the two different representations of the bulk fluid. Fig. 2 illustrates how to interface two SDPD fluids with different levels of detail for the case of large particles twice as massive as the fine particles, where the large particles therefore split into twos. The interface region is itself divided into three separate subdomains (1) an overlap region, (2) a coarsening region, and (3) a refining region. Particles in the system are free to traverse the interface and mass transfer between domains with different resolutions is unrestricted. Mass is conserved through particle splitting and combining when moving across this boundary.

If a large SDPD particle is transported into the interface region, either due to advection or Brownian motion, and then eventually moves into the refining subregion, it splits into two small SDPD particles. Here, we have assumed that the small SDPD particles in the finely resolved part of the simulation box have half the mass of the large particles in the coarse region, $m_2 = 2m_1$. It is possible to generalize this kind of approach for situations where the massive particles are n times more massive than the small particles, where n is an integer greater than one, and hence large particles can split into n smaller particles. For simplicity, we assume $n = 2$. The remaining splitting rules are constructed such that momentum and the amount of solute are also conserved. Note that there are multiple ways to assign new positions to the daughter particles upon splitting. In the work of Backer et al.,[71] both particles are inserted at the same location as the

parent particle. Due to the soft DPD interactions, the system remains stable in spite of both particles occupying the same point, and the thermostat dissipates heat generated due to particle overlap after the insertion. However, for fluids with quasi-incompressible equations of state, this heating may be substantial. Therefore, Kulkarni et al. adopt an alternative perspective where both particles are inserted randomly inside a region that corresponds to the influence domain of the parent particle (i.e., within a sphere surrounding the parent particle with radius equal to the parent's smoothing length). This reduces the problem of heating, although the center of mass of the original particle is no longer conserved.

Here, we take a different approach and only insert one of the two daughter particles randomly inside the parent particle's influence domain. After particle j is inserted at random inside a sphere with radius h_i surrounding the parent particle i, the second particle k is inserted at a position such that the center of mass of the parent particle is preserved. In other words, if a large particle i splits into small particles j and k, we generate a random displacement vector $\Delta \mathbf{r}_{ij} = \mathbf{r}_i - \mathbf{r}_j$ according to $\Delta \mathbf{r}_{ij} = random(h_i)$. Then, the appropriate rules are

$$
\begin{aligned}
m_j &= m_k = 0.5 m_i, \\
\mathbf{v}_j &= \mathbf{v}_k = \mathbf{v}_i, \\
\mathbf{r}_j &= \mathbf{r}_i - \Delta \mathbf{r}_{ij}, \\
\mathbf{r}_k &= \mathbf{r}_i + \Delta \mathbf{r}_{ij}, \\
\Phi_j &= \Phi_k = \Phi_i.
\end{aligned}
\tag{32}
$$

This procedure also ensures that potential energy is conserved in simulations that feature a linear external potential acting on the particle masses (e.g., gravity). We have tested the procedure implied by Eq. (32) by placing two fluids with different resolutions next to a wall in a semi-infinite domain, with a uniform gravitational force in the direction of the wall. The computed density profiles do in fact show the correct equilibrium Boltzmann distribution, without artifacts due to the interface. Moreover, this test is successful whether or not

the more massive-particle fluid is on top or bottom. (Detailed results are not shown here.)

The rules for combining smaller particles into larger ones are more straightforward. If a small particle j is transported to the interface region and crosses into the coarsening region, the nearest small particle k is located, and the two are combined into large particle i using the following rules:

$$
\begin{aligned}
m_i &= m_j + m_k, \\
\mathbf{v}_i &= 0.5\left(\mathbf{v}_j + \mathbf{v}_k\right), \\
\mathbf{r}_i &= 0.5\left(\mathbf{r}_j + \mathbf{r}_k\right), \\
\Phi_i &= 0.5\left(\Phi_j + \Phi_k\right).
\end{aligned}
\tag{33}
$$

We note that with the particle splitting and combining steps in this top-down multiscale approach, it is not strictly possible to satisfy detailed balance because the coarsening and refining subregions, where the "forward" and "reverse" moves take place, are spatially separated. However, this splitting/combining scheme maintains conserved physical quantities and has been shown to accurately reproduce hydrodynamic behavior.[31,71] For the single-component case, this method yields a flat density distribution at equilibrium, as well as accurate solutions for the flow field in simple problems such as shear flow. Specifically, Backer *et al.* consider cases where the flow is both perpendicular and parallel to the interface separating the regions with different resolutions, and in both cases, there is good agreement of the numerical result with the analytical solution from Navier-Stokes.

In this section and Sec. VI, we benchmark the multiscale multicomponent approach by performing simple equilibrium and non-equilibrium problems. Due to the presence of multiple length scales, a few additional details require discussion. Note that previously it was possible to hold the smoothing length constant for all particles. In the present multiscale scenario where the fluid resolution changes with position, the smoothing length for every particle must be allowed to vary since the number density varies in space, and each particle must maintain the appropriate number of nearest neighbors. Thus, each particle is assigned a smoothing length variable that is updated at each time-step based on the local SDPD particle number density,[31]

$$
h_i = h_0 \nu_i^{-1/3}.
\tag{34}
$$

Here, ν_i is the local number density computed from $\nu_i = \sum_j W_{ij}$. h_0 is a constant parameter selected so that each particle has ~56 neighbors within its own influence domain, which is required for the accuracy of the particle approximation.[57] In this work, we choose $h_0 = 1.2$.[31,57] In order to ensure symmetric interactions, we use the arithmetic mean of particle smoothing lengths when computing pair interactions, $h_{ij} = \left(h_i + h_j\right)/2$.

Unlike previous studies that only focused on single-component systems, Eqs. (32) and (33) include the appropriate splitting and combining rules for a binary mixture. We confirm that this approach reproduces correct equilibrium properties uniformly across the simulation box by considering a fluid at reduced temperature $T = 1$ with density $\rho = 0.8$ and viscosities $\eta = 1.9$ and $\zeta = 0.9$. Initially, we divide the global simulation box (with volume $50 \times 50 \times 100$) into

two parts, with 1000 fine particles in the region located at $z < 50$ and 512 coarse particles in the region at $z > 50$. The fine particles are initialized on a $10 \times 10 \times 10$ lattice inside a $50 \times 50 \times 50$ volume. These "fine" particles have mass $m = 100$ and smoothing length $h = 6.0$. For the coarse region, particles are initially placed on an $8 \times 8 \times 8$ lattice inside a volume with dimensions $50 \times 50 \times 50$. These "coarse" particles have a mass of $m = 200$ and smoothing length $h = 7.5$. The z-coordinate is perpendicular to the interface separating the coarse and fine SDPD domains [see Fig. 3(a)]. Periodic boundary conditions are used in all directions. The interface regions have a width of 9.0 and are located between $z = 0.0$ and 9.0, and $z = 50.0$ and 59.0. It is necessary to include two transition zones due to the periodicity of the simulation box. Each of the interface coarsening, refining, and overlap subdomains has a width of 3.0. The interface region should be sufficiently large to allow for a smooth transition of the smoothing length; when an inadequately sized transition region is used, particles near the interface have a different number of neighbors from particles in the bulk, which can result in unphysical density gradients.[71] After initializing positions, all the particles are translated in the z-direction by half the interface region width so that the initial boundary between the coarse and fine particle lattices is located precisely half-way inside the interface regions, within the overlap subdomains ($z = 4.5$ and $z = 54.5$). We use a time step of $\Delta t = 0.001$ and collect data for 5×10^6 steps after equilibrating for 1×10^6. Five cases with average concentrations $\langle \Phi \rangle = 0.25$, 0.40, 0.50, 0.60, and 0.75 are
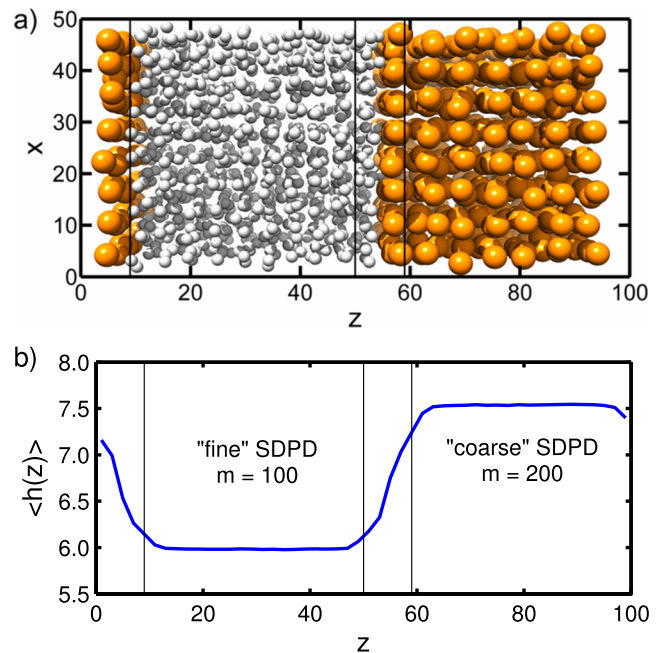

FIG. 3. (a) Visualization of equilibrium multiscale SDPD simulation. The left bulk region (white particles) is the finely resolved SDPD fluid with smoothing length $h = 6.0$, and the particles on the right (orange) are the coarse ones with $h = 7.5$. These coarse particles are twice as massive as the fine ones, and their number density is half as much. Periodic boundary conditions are used for the x-, y-, and z-directions. (b) The corresponding smoothing length versus position for an equilibrium multiscale SDPD simulation. The interface regions are located between $z = 0.0$ and 9.0 and between $z = 50.0$ and 59.0.

considered. The neighbor list is updated every ten steps, unless the number of particles in the system changes due to splitting/combining of particles, in which case it is also rebuilt.

The system is illustrated in Fig. 3(a), and the smoothing length as a function of position is obtained from a binning procedure and shown in Fig. 3(b). The regions where the smoothing length is low ($h = 6.0$) contain particles with mass $m = 100$, and the part where $h = 7.5$ features particles with mass $m = 200$, with a smooth transition between the two values of h across the interface separating the two domains. Fig. 4(a) gives the concentration profiles for the five different average concentrations investigated. There are no unphysical concentration gradients perpendicular to the interface between the fine and coarse regions, and the distribution of solute is uniform. The average error per bin in the profiles across all five cases is 0.0003%. We also compare the concentration distributions in the fine and coarse regions to the exact analytical result [Eq. (31)] in Fig. 4(b) and find that both the finely resolved and coarse-grained regions in the multiscale simulation exhibit fluctuations in concentration appropriate for their respective scales. The distributions for the $\langle \Phi \rangle = 0.40$ and 0.60 are omitted for clarity.

VI. ONE-DIMENSIONAL DIFFUSION ACROSS MULTIPLE LENGTH SCALES

Next, we demonstrate that our multiscale multicomponent method captures diffusion dynamics correctly across multiple length scales by performing a multiscale simulation of quasi-1D diffusion. Once again, we choose $T = 1$ and $\rho = 0.8$ as the state point, and $D = 1.0$, $\zeta = 0.9$, and $\eta = 1.9$ for the transport coefficients. The system is set up as follows: the global simulation box has dimensions $50 \times 50 \times 200$, where one side initially contains 2000 fine particles, and the other side contains 1024 coarse particles. At the start of the simulation, the finely resolved particles are initialized on a $10 \times 10 \times 20$ lattice inside a region with dimensions $50 \times 50 \times 100$, which is a subset of the whole simulation box. These particles have a mass of 100 and smoothing length of 6.0. Next to this region, we initialize the coarse SDPD particles (with mass of 200 and smoothing length of 7.5) on an $8 \times 8 \times 16$ lattice inside a part of the global simulation box with dimensions $50 \times 50 \times 100$. The vector normal to the interface separating the coarse and fine regions is in the z-direction. The interface region separating the coarse and fine domains has a width of 9.0 and is centered at $z = 100$. The simulation box features periodic boundary conditions in the x- and y-directions. The
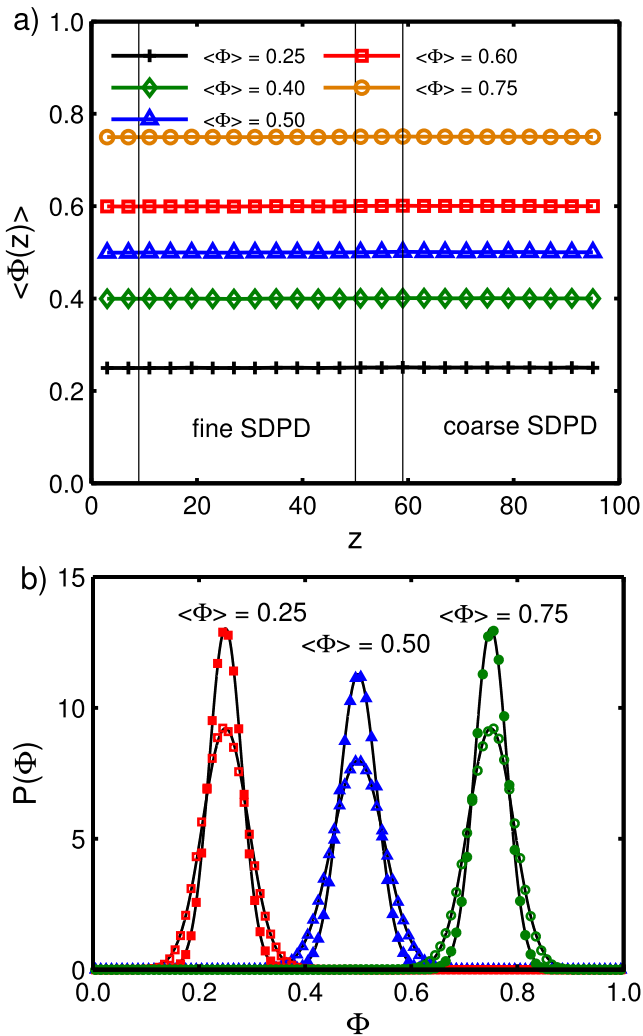

FIG. 4. (a) Concentration profiles for equilibrium multiscale SDPD simulations. We have performed tests at several different average concentrations, $\langle \Phi \rangle = 0.25, 0.40, 0.50, 0.60$, and 0.75, where the results from each simulation are shown with a different marker/color. (b) Concentration probability distributions from equilibrium multiscale simulations. For clarity, we show results for three of the five cases: $\langle \Phi \rangle = 0.25$ (red/square markers), 0.50 (blue/triangle markers), and 0.75 (green/circle markers). The solid markers represent the probability distribution in the "coarse" SDPD region, and the hollow markers represent the "fine" SDPD region. The black curves are the exact analytical solution. The distributions for $\langle \Phi \rangle = 0.40$ and 0.60 are omitted for clarity.
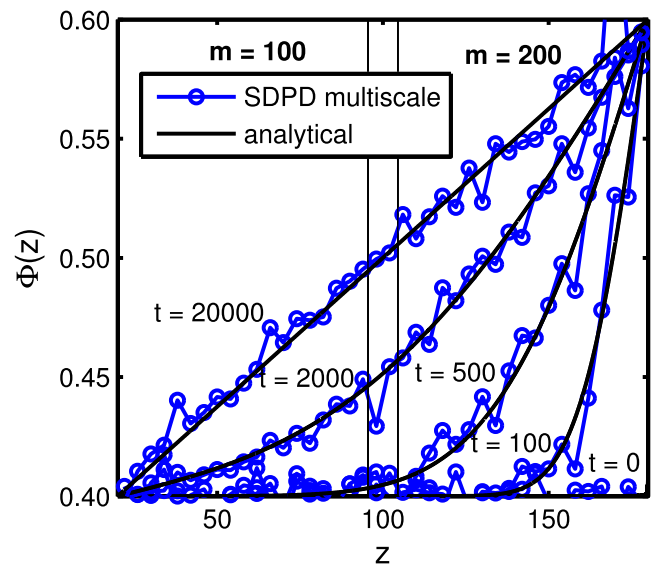

FIG. 5. Concentration profile at different times for the quasi-one-dimensional diffusion problem across multiple length scales. A fluid region is situated between two walls, and the fluid itself is divided into finely resolved and coarse-grained domains, where particles have masses $m = 100$ and $m = 200$, respectively. After equilibrating, a concentration gradient is imposed by holding the concentration fixed at 0.4 at the left boundary and 0.6 at the right boundary, and the time-evolution of the concentration profile is computed. The numerical results (blue curve and circle markers) are shown against the exact solution of the non-fluctuating diffusion equation (black curve).

walls are located $z = 20$ and $z = 180$, and particles located at $z < 20$ and $z > 180$ are labelled as virtual particles; their positions and concentrations are not evolved in time. The fluid particles are initialized with an average concentration of 0.4. We use a time step of $\Delta t = 0.01$ and equilibrate for 1×10^6 time-steps.

After equilibration a concentration gradient is imposed on the system by increasing the concentration of the wall particles located at $z > 180$ to 0.6. Boundary conditions are enforced using the approach described in Section III. The gradient is perpendicular to the interface separating the fine and coarse regions and hence drives solute transfer across the boundary from the region with coarse resolution to the finely resolved SDPD region. The resulting transient concentration profile is shown for several different times and compared to the exact analytical solution of the non-fluctuating diffusion equation in Fig. 5. The results show excellent agreement with the exact solution, mass transfer is correctly mediated across domains with different levels of detail, and diffusion is independent of the degree of coarse-graining. At steady-state, the time-averaged concentration profile is perfectly linear and does not exhibit unphysical artifacts due to the interface between the two SDPD regions with different resolutions.

VII. CONCLUSION

In this work, we provide a new multiscale fluctuating continuum particle approach for ideal solutions. The stochastic differential equations governing the concentration field are obtained by introducing thermal noise in the Lagrangian SPH equation for diffusion using the GENERIC formalism. Random fluxes of solute are pairwise between particles and constructed such that fluctuation-dissipation is satisfied. When solved concurrently with the SDPD equations of motion, this set of SDEs allows for treatment of advection-diffusion problems across length scales ranging from nanometers to microns and the non-fluctuating continuum limit. The characteristic length scale of the fluid is controlled by the smoothing length parameter, which influences both the distribution of momenta and solute concentrations. We illustrate that this new multicomponent SDPD reproduces the correct fluctuations by performing equilibrium simulations at different average concentrations and resolutions (i.e., smoothing lengths). In all cases, the results show excellent agreement with the analytical result for the probability distribution of concentrations.

Importantly, the ability to control the smoothing length parameter makes multicomponent SDPD ideal for multiscale simulation. Thus, we use this approach to extend the single-component multiscale SDPD techniques of Kulkarni *et al.* to binary solute-solvent systems and propose refining and coarsening rules for particle splitting/combining such that mass, momentum, and solute are conserved. In order to validate this framework for multicomponent multiscale simulation, we perform equilibrium simulations involving SDPD fluids with different degrees of coarse-graining and demonstrate that there are no unphysical artifacts in the concentration profile near the interface between the two regions, and each region features the appropriate fluctuations

for its corresponding length scale. Finally, we apply these tools to a simple non-equilibrium problem (one-dimensional diffusion across a narrow channel), and we demonstrate that this multiscale method correctly captures the propagation of a concentration gradient across multiple length scales and accurately reproduces the expected diffusion dynamics with solute transfer from the coarse region to the fine one.

The presented multiscale multicomponent approach does have a number of limitations, however. First, for very small SDPD particles with concentration close to zero or unity such that the analytical Gaussian distribution of concentrations is truncated, precision issues can lead to unphysical negative concentrations (or concentrations greater than one). It is possible to remedy this problem either by reducing the time-step or by using a dynamic time-step approach, such as the Brownian tree algorithm described in Ref. 70. Second, the method is based on a discretization of the diffusion equation, which is relevant to a very wide range of different problems, but which ultimately assumes ideal mixing. Moreover, constant temperature conditions and a quasi-incompressible fluid are also assumed. These simplifications may be relaxed, although the resulting equations of motion become more complex and for the case of temperature gradients, it is necessary to solve the entropy equation in addition to the ones for momentum and solute diffusion. Finally, while this approach provides a basis for coarse-graining regions where a high level of detail is unnecessary, it is still purely a continuum approach. The power of this framework lies in the ability to reduce the number of particles in bulk regions where high detail is not required, lowering computational cost. However, for certain problems, it may be necessary to retain atomistic resolution in select regions to capture important effects. In a prior study, we developed an approach for embedding a MD region inside a coarse-grained SDPD fluid, and constructing these kinds of MD-SDPD hybrid approaches for multicomponent systems will be the subject of future work.

[1]P. Español and M. Revenga, Phys. Rev. E **67**, 026705 (2003).
[2]S. Litvinov, X. Y. Hu, and N. A. Adams, J. Phys. Condens. Matter **23**, 184118 (2011).
[3]A. Vázquez-Quesada, M. Ellero, and P. Español, J. Chem. Phys. **130**, 034901 (2009).
[4]N. Moreno, P. Vignal, J. Li, and V. M. Calo, Procedia Comput. Sci. **18**, 2565 (2013).
[5]K. Müller, D. A. Fedosov, and G. Gompper, Sci. Rep. **4**, 4871 (2014).
[6]X. Bian, S. Litvinov, R. Qian, M. Ellero, and N. A. Adams, Phys. Fluids **24**, 012002 (2012).

[7] A. Vázquez-Quesada, M. Ellero, and P. Español, Phys. Rev. E **79**, 056707 (2009).

[8] M. Ellero, P. Español, and E. G. Flekkøy, Phys. Rev. E **68**, 041504 (2003).

[9] C. Thieulot, L. P. B. M. Janssen, and P. Español, Phys. Rev. E **72**, 016713 (2005).

[10] C. Thieulot, L. P. B. M. Janssen, and P. Español, Phys. Rev. E **72**, 016714 (2005).

[11] M. Grmela and H. C. Öttinger, Phys. Rev. E **56**, 6620 (1997).

[12] H. C. Öttinger and M. Grmela, Phys. Rev. E **56**, 6633 (1997).

[13] H. C. Öttinger, *Beyond Equilibrium Thermodynamics* (Wiley-Interscience, Hoboken, NJ, 2005).

[14] P. V. Coveney and P. Español, J. Phys. A: Math. Gen. **30**, 779 (1997).

[15] M. Laradji and M. J. A. Hore, J. Chem. Phys. **121**, 10641 (2004).

[16] Z. Li, A. Yazdani, A. Tartakovsky, and G. E. Karniadakis, J. Chem. Phys. **143**, 014101 (2015).

[17] J. Kordilla, W. Pan, and A. Tartakovsky, J. Chem. Phys. **141**, 224112 (2014).

[18] L. D. Landau and E. M. Lifshitz, *Fluid Mechanics*, 2nd ed. (Butterworth-Heinemann, Amsterdam, 1987), Vol. 6.

[19] C. Cohen, J. W. H. Sutherland, and J. M. Deutch, Phys. Chem. Liq. **2**, 213 (1971).

[20] J. M. O. de Zarate and J. V. Sengers, *Hydrodynamic Fluctuations in Fluids and Fluid Mixtures*, 1st ed. (Elsevier Science, 2006).

[21] S. T. O'Connell and P. A. Thompson, Phys. Rev. E **52**, R5792 (1995).

[22] N. G. Hadjiconstantinou and A. T. Patera, Int. J. Mod. Phys. C **08**, 967 (1997).

[23] N. G. Hadjiconstantinou, J. Comput. Phys. **154**, 245 (1999).

[24] X. B. Nie, S. Y. Chen, W. N. E., and M. O. Robbins, J. Fluid Mech. **500**, 55 (2004).

[25] R. Delgado-Buscalioni and P. V. Coveney, Phys. Rev. E **67**, 046704 (2003).

[26] R. Delgado-Buscalioni and G. De Fabritiis, Phys. Rev. E **76**, 036709 (2007).

[27] R. Delgado-Buscalioni, K. Kremer, and M. Praprotnik, J. Chem. Phys. **128**, 114110 (2008).

[28] D. A. Fedosov and G. E. Karniadakis, J. Comput. Phys. **228**, 1157 (2009).

[29] I. Korotkin, S. Karabasov, D. Nerukh, A. Markesteijn, A. Scukins, V. Farafonov, and E. Pavlov, J. Chem. Phys. **143**, 014110 (2015).

[30] N. D. Petsev, L. G. Leal, and M. S. Shell, J. Chem. Phys. **142**, 044101 (2015).

[31] P. M. Kulkarni, C.-C. Fu, M. S. Shell, and L. Gary Leal, J. Chem. Phys. **138**, 234105 (2013).

[32] P. J. Atzberger, J. Comput. Phys. **229**, 3474 (2010).

[33] P. J. Hoogerbrugge and J. M. V. A. Koelman, Europhys. Lett. **19**, 155 (1992).

[34] P. Español and P. Warren, Europhys. Lett. **30**, 191 (1995).

[35] P. Español, Phys. Rev. E **52**, 1734 (1995).

[36] Y. Kong, C. W. Manke, W. G. Madden, and A. G. Schlijper, Int. J. Thermophys. **15**, 1093 (1994).

[37] Y. Kong, C. W. Manke, W. G. Madden, and A. G. Schlijper, J. Chem. Phys. **107**, 592 (1997).

[38] W. Jiang, J. Huang, Y. Wang, and M. Laradji, J. Chem. Phys. **126**, 044901 (2007).

[39] P. Nikunen, I. Vattulainen, and M. Karttunen, Phys. Rev. E **75**, 036713 (2007).

[40] E. S. Boek, P. V. Coveney, H. N. W. Lekkerkerker, and P. van der Schoot, Phys. Rev. E **55**, 3124 (1997).

[41] A. Chatterjee and L.-M. Wu, Mol. Simul. **34**, 243 (2008).

[42] R. D. Groot, J. Chem. Phys. **136**, 064901 (2012).

[43] D.-W. Li and X. Y. Liu, J. Chem. Phys. **122**, 174909 (2005).

[44] A. Grafmüller, J. Shillcock, and R. Lipowsky, Phys. Rev. Lett. **98**, 218101 (2007).

[45] L. Rekvig, M. Kranenburg, J. Vreede, B. Hafskjold, and B. Smit, Langmuir **19**, 8195 (2003).

[46] S. Yamamoto, Y. Maruyama, and S. Hyodo, J. Chem. Phys. **116**, 5842 (2002).

[47] M. Laradji and P. B. Sunil Kumar, Phys. Rev. Lett. **93**, 198105 (2004).

[48] D. Reith, M. Pütz, and F. Müller-Plathe, J. Comput. Chem. **24**, 1624 (2003).

[49] M. S. Shell, J. Chem. Phys. **129**, 144108 (2008).

[50] A. P. Lyubartsev, M. Karttunen, I. Vattulainen, and A. Laaksonen, Soft Mater. **1**, 121 (2002).

[51] T. Soddemann, B. Dünweg, and K. Kremer, Phys. Rev. E **68**, 046702 (2003).

[52] C.-C. Fu, P. M. Kulkarni, M. S. Shell, and L. G. Leal, J. Chem. Phys. **139**, 094107 (2013).

[53] C. A. Marsh, G. Backx, and M. H. Ernst, Phys. Rev. E **56**, 1676 (1997).

[54] M. Ripoll, M. H. Ernst, and P. Español, J. Chem. Phys. **115**, 7271 (2001).

[55] L. B. Lucy, Astron. J. **82**, 1013 (1977).

[56] R. A. Gingold and J. J. Monaghan, Mon. Not. R. Astron. Soc. **181**, 375 (1977).

[57] G. R. Liu and M. B. Liu, *Smoothed Particle Hydrodynamics: A Meshfree Particle Method* (World Scientific Publishing Company, 2003).

[58] J. P. Morris, P. J. Fox, and Y. Zhu, J. Comput. Phys. **136**, 214 (1997).

[59] S. R. D. Groot and P. Mazur, *Non-Equilibrium Thermodynamics*, Dover ed. (Dover Publications, New York, 2011).

[60] J. J. Monaghan, Rep. Prog. Phys. **68**, 1703 (2005).

[61] J. J. Monaghan, Comput. Phys. Rep. **3**, 71 (1985).

[62] P. Español, Phys. Rev. E **57**, 2930 (1998).

[63] A. Donev, J. B. Bell, A. de la Fuente, and A. L. Garcia, J. Stat. Mech.: Theory Exp. **2011**, P06014.

[64] L. D. Landau, E. M. Lifshitz, and L. P. Pitaevskii, *Statistical Physics Part 1*, 3rd ed. (Butterworth-Heinemann, Oxford, England, 1980).

[65] A. Donev, J. B. Bell, A. de la Fuente, and A. L. Garcia, Phys. Rev. Lett. **106**, 204501 (2011).

[66] K. Meier, A. Laesecke, and S. Kabelac, J. Chem. Phys. **122**, 014513 (2005).

[67] K. Meier, A. Laesecke, and S. Kabelac, J. Chem. Phys. **121**, 3671 (2004).

[68] P. E. Kloeden and E. Platen, *Numerical Solution of Stochastic Differential Equations* (Springer, Berlin, 2010).

[69] R. D. Groot and P. B. Warren, J. Chem. Phys. **107**, 4423 (1997).

[70] V. Sotiropoulos and Y. N. Kaznessis, J. Chem. Phys. **128**, 014103 (2008).

[71] J. A. Backer, C. P. Lowe, H. C. J. Hoefsloot, and P. D. Iedema, J. Chem. Phys. **123**, 114905 (2005).